Measurement of Laminar Burning Speed and Investigation of Flame Stability of Syngas/Air Mixture

A Thesis presented

by

Bander Nafe Alhazmi

to

The Department of Mechanical and Industrial Engineering

In partial fulfillment of the requirements

for the degree of

Master of Science

in

Mechanical Engineering

in the field of

Thermo-fluids

Northeastern University

Boston, Massachusetts

April 2015

ABSTRACT

Synthetic gas (Syngas) is a growing alternative fuel for fossil fuel used in power generation industries. It is cost effective and friendly with the ecosystem. In order to validate its capability as fuel supply, determination of syngas laminar burning speed is fundamental to understand its combustion behavior and kinetic model. Laminar burning speed of syngas with 5% of hydrogen and 95% carbon monoxide mixture has been measured using a constant volume cylindrical chamber and schlieren photography. The laminar burning speed has been measured in the range of temperature from 315 K to 490 K and range of pressure from 0.5 atm to 3.2 atm. The equivalence ratios for the combustible mixture ranged from 0.6 to 5. The thermodynamic model for calculating the laminar burning speed is based on the pressure rise method considering energy losses to the ignition source, unburned gas and chamber wall. The structure of the flame was studied through the shadowgraph method. Laminar burning speeds have only been reported for smooth flame. The results indicated that the laminar burning speed increases with increasing temperature and decreases as pressure increases. Flame cellularity was found to develop at early stage at high initial pressures. The measured burning speed has been compared with other researchers' data and the results were in a good agreement.

ACKNOWLEDGEMENTS

I would like to express my appreciation and gratitude to my advisor Professor Hameed Metghalchi. His positivity and encouragement through all this journey have empowered me to overcome difficult times. He has always been a great teacher and a friend. Thank you for giving me the opportunity to work under your supervision. Also, I would like to thank my laboratory colleagues Alden Ahlholm, Omid Askari, and Ali Moghaddas for being such a wonderful group to work with.

Finally, I would like to thank my family for their unconditional support and patience to help me achieve this goal. I could have not made it without them.

TABLE OF CONTENTS

LIST OF FIGURES

LIST OF TABLES

1. Introduction

The compelling need to identify an alternative fuel that meets global demands and be harmless to the ecosystem derived scientists and experimentalists to explore unconventional sources of energy. Among those sources of energy is the synthetic gas (syngas). Since the inception of syngas, researchers have explored its kinetics and thermodynamic properties. As advantageous as being synthesized by various sources and through different methods, syngas production varies greatly in chemical structure. That is its basic constituents amalgamate with different molar ratios in addition to the inclusion of other species. As a result, the available studies are less than adequate to aver the syngas thermodynamic and thermophyscial properties as well as its combustible behavior. Hence, this research has been carried out to further study the syngas combustible behavior at various conditions ranging from lean to rich mixture, sub-atmospheric and elevated pressure and at higher temperature.

A profound thermophysical property that is a building block to form the syngas kinetic scheme and understand its combustible behavior is laminar burning speed. During combustion of fuel-oxidizer mixture, the ignition source will result into explosive reaction zone that would consequently propagate through the remaining unburned flammable mixture. The propagation of the explosive zone is also called combustion wave or propagation wave [1]. The speed of this propagation wave outwardly normal to the flame surface and relative to the unburned gas is the laminar burning speed [2]. The burning speed is bounded by the heat conduction and diffusion of active particles at the boundary of the burned mixture and the unburned mixture [1].

Understanding the laminar burning speed evolved through theoretical analysis and experimental studies due to its complexity. The following sections shares insight into those two approaches.

1.1. Theoretical Approach

The historical development to analytically calculate the burning speed is initiated by the thermal theorem as proposed by Mallard and LeChatelier. The core assumption of the theory is separating the fuel-oxidizer mixture into reaction zone and preheat zone and only considering energy transfer by conduction to the unburned mixture [1,2]. As the mass of the mixture can be represented by the density and the speed of the mixture and that the reaction region's thickness may be related to the reaction rate and time, they deduce that the laminar burning speed is proportional to the square root of the rate of reaction evaluated at the burning temperature [1,2].

Later Zel'dovich, Frank-Kamenetskii and Semenov introduced the diffusion theory [1,2]. In addition to the heat effect, they considered the diffusion of molecules but excluded radicals and atoms [2]. The diffusion theory is more focused on the heat transported by the species. It was assumed that the terms related to the reaction region are insignificant compared to the preheated zone. The assumption included that the heat conduction by the chemical reactions in the reaction zone is the major contributor resulting in neglecting the participation of convective heat transfer [1]. In addition, they limited their analysis to a constant total molar number of the reactant and unity value of Lewis number (ratio of thermal diffusion to mass diffusion) conditions [1,2]. To eliminate the ignition temperature from their calculation they assumed that all the reaction will take please near the flame temperature, hence, replacing the ignition temperature with flame temperature.

Later in the development of this theory, radical particles and low atomic weight molecules were considered critical for the burning reaction.

Finally, the third analytical approach is the comprehensive theory. The comprehensive theory invokes the conservation equations of mass, momentum and energy and the diffusion equation. There are many attempts to obtain solutions for these equations. Noteworthy solution is the consideration eigenvalue problems and assuming that the eigenvalue is the same for all equations considering all the ranges of ignition temperature. Another solution is considering a heat sink at the boundary that is at the wall quench layer [1,2].

1.2. Experimental Approach

Various experimental setups were designed to elucidate physical, thermophyscial and chemical effects on the flame structure and patterns. The following are the most common methods used for experimentation. These methods can be generalized into stationary flame and propagating flame.

1.2.1. Stationary Flame

In this category of setups, the flame is stationary, while the premixed mixture approaches with laminar speed. Common used methods are Bunsen burner and flat-flame methods [1,3]. Using Bunsen burner method, the premixed combustible mixture approaches the stationary flame through long cylindrical tube or nozzle. The passage of the mixture is designed to maintain uniform streamline flow. At the exit of the tube, the mixture is burned and creates a Bunsen cone shape. The flame geometry is measured and studied with several developed techniques. Since the flame is stationary the burning velocity on the flame front would be the same as the gas velocity normal to the flame surface area.

Using mass continuity equation is another method of determining the burning speed in this setup. Burning mass rate divided by the average unburned gas density and flame front area results into the average burning speed. A more rigorous approach is by invoking the conservation of momentum equation. Here the pressure difference across the flame front can yield the calculation of burning speed. The Bunsen burner method has couple of disadvantages that would affect the validity of the results. The main issues are non-uniformity of burning velocity over the flame surface due to the gradient of the flame temperature, difficulty to maintain uniform gas flow and the inaccuracy of assuming adiabatic flame due to the heat losses near the nozzle outlet [1-3].

For the flat-flame method, the mixture enters a mixing chamber to ensure homogeneity and then passes through series of matrices or porous metal disks to ensure even distribution and laminar flow. Consequently, the mixture enters a cylindrical burner initially with high flow rate and then is adjusted for reaching flat flame. As the volumetric flow rate can be fairly accurately measured the burning speed can be obtained by dividing the volumetric flow rate by the flat flame diameter. However, this method can only be used for low burning velocity of up to 1 m/s. The uncertainty of the results lies in the potential of escaped unburned gas form the burner, energy losses from the burner and the preheating by the matrix [1-3].

1.2.2. Propagating Flame

Propagating flame is based on igniting a quiescent mixture usually centrally and as a result the flame propagates outwardly through the unburned mixture. This method relies on either constant pressure or volume. Known methods are spherical constant volume chamber, soap bubble, and cylindrical tube methods [1,3].

The spherical bomb setup is based on constant volume. It contains quiescent and homogeneous mixture that is centrally ignited. The pressure variation with time is key data to obtain the burning speed through various developed correlation [1-3]. Further details of this method will be explained in the experimental setup of this document.

In the soap bubble method, the combustible mixture is ignited at the center. As result, the flame propagates outwardly resulting in increased volume, while the pressure remains constant during the process. A shadowgraph optical recoding is employed to identify the spatial velocity. By the knowledge of the spatial velocity along with the expansion ratio, the burning speed can be determined. The uncertainty lies in the ratio of the initial temperature to the flame temperature as well as the density ratio [1-3].

For the tube method, the mixture placed into a horizontal tube. The tube is opened from one end while the other is closed. The mixture is ignited from the open end and the progression of flame towards the closed end is the burning speed [1-3].

2. Synthetic Gas (Syngas)

2.1. Background

Power and energy industries are being under increasing pressure to explore new facet of fuel that can replace conventional fuel sources such as fossil fuel. Pressure arises from the environmental friendly perspective and sustainability concerns to meet global demands. Driven by these challenges, scientists have studied and proposed several fuel alternatives among which is syngas. Syngas has prosperous future due to the abundance of its sources and versatility in its application. Syngas can be produced from natural gas through steam reforming process and coal and bio-waste through gasification [4]. Currently, syngas is produced from coal, fossil fuel residues and biomass [5]. This fuel can be used directly as source of energy in gas turbines, fuel cells, and integrated gasification combined cycles (IGCC) power plants. Employing Fischer-Tropsch synthesis, syngas can yield production of synthetic petroleum.

Techniques for producing syngas have evolved to be economically feasible and yield cleaner and higher calorific fuel. However, versatility of synthesizing the fuel laid down further challenge of inconsistent syngas composition. Syngas is constituted of mainly Hydrogen (H_2) and carbon monoxide (CO) along with other compounds such as Nitrogen (N_2), methane (CH_4), carbon dioxide (CO_2) and to less extent heavier Hydrocarbons. The ratio of hydrogen to carbon monoxide as well as inclusion of other substances relies on the method and source being used [4,5].

The challenge in the use of syngas in power industries is exhibited in clean production of the fuel and the composition of its basic constituents. Gasification produces syngas with undesired products such as NH_3 and H_2S, which upon combustion produce pollutant,

NOx and SOx respectively [4]. The variation of hydrogen to carbon monoxide ratio leads to difficulty of understanding the kinetic and combustion behavior of the fuel. This ratio's inconstancy broadens the study conditions for understanding the combustion of syngas. Researchers have explored the fuel for various H_2/CO ratios at different pressure, temperature, and equivalence ratio as well as the inclusion of diluents.

2.2. Literature Studies of Syngas

Considering 50:50 ratio of hydrogen (H_2) and carbon monoxide (CO), Yang Zhang et al. [6] conducted burning speed measurement for syngas under lean mixture conditions for atmospheric pressure and ambient temperature using twin flame, opposite jet counterflow method. The experiment was ranged from 0.4 to 0.7 equivalence ratios. The authors [6] noted that the laminar burning speed increased fast when hydrogen ration is less than 15%. While the burning speed increased almost linearly at higher hydrogen content than 15%. The burning speed and flame structure of syngas with increased H_2 concentration with roughly 6% than CO resemble more closely the behavior of pure hydrogen than that of the CO mixture [7].

Also Bouvet et al. [8,9] experimented syngas laminar burning speed with various ration of H_2/CO using straight burners setup with flame surface and Bunsen burner methods. Hydrogen mixtures of 1% to 100% with equivalence ratios ranging from 0.3 to 1.2 were investigated. Similar conclusion was observed compared to Yang Zhang et al. [6] and other experiment results. Bouvet et al. [8,9] indicated that the burning speed is proportional to the increase of the hydrogen content, while the speed behaves linearly in lean mixture. Moreover, the results were compared with prediction models. Bouvet et al. results depicted an agreement with of Sun et al. [10] and Li et al. [11] model for 50%

hydrogen content. However, while Silvaramakrishnan et al [12] and Davis et al. [13] models were offset with the 50% hydrogen results of Bouvet et al [8], discrepancies decreases as the hydrogen percentage decrease in the mixture. Also, Bouvet et al. [14] conducted syngas laminar burning speed tests using constant volume outwardly spherical propagation method for 5-50% H_2 blends and 0.4-5 equivalence ratios at ambient temperature and atmospheric pressure. There was general agreement of the result with some previous studies for lower equivalence ratios of up to 2.5 for the cases of 5%, 10% and 25% H_2.

Chen Dong et al. [15] explored the laminar burning speed using Bunsen burner method with wide range of hydrogen mixture 10% to 100% and fuel-air ratio 0.7-2.1 at atmospheric pressure and room temperature. Comparing the burning speed patterns were compared with the increase of hydrogen and carbon monoxides ratios increase, the laminar burning speed corresponds much rapidly with the increase of hydrogen (H_2) than carbon monoxide (CO). Similar to Yang Zhang et al. [6] and Bouvet et al. [8,9], Chen Dong et al. [15] indicated that burning speed rapidly increase below 20% H_2 ratio and linearly increase with higher fractions. In addition, Chen Dong et al. [15] argued that the burning speed higher than 80% H_2 turns back to rapid increment.

In studying the effect of pressure on the syngas laminar burning speed, Lui et al. [16] examined the fuel combustion at range of pressures 0.1-1.0 MPa and fuel-air equivalence ratios between 0.5-0.7. Using outwardly spherical flame propagation technique, the results [16] suggested that the laminar burning speed decreases with the increase of pressure for both equivalence ratios. At higher pressure, the hydrodynamic instability gets elevated resulting in higher probability of cellular formation at small radii.

Illustrating further the pressure effect on syngas burning speed, Lui et al. [16] compared the combustion behavior in lean combustion with that of the methane fuel. Comparison revealed that the increase of pressure has less effect on syngas combustion than that of the methane. The authors [16] referred the reasons to the complexity of the oxidation route by which reaction rate decreases. At elevated pressure, HO_2-containing reaction becomes more significant, hence, unlocking additional route for the CO oxidation that competes with the original oxidation route of hydrogen with oxygen [16].

Diluents play major role in the flame stability and corresponding values of the buring speed. Prathap et al. [7] studied the effect of diluent using Nitrogen (N_2) on the syngas laminar burning speed. They used 50:50 ratio of H_2/CO at 0.1 MPa, 300K, while varying fuel-air ratios from 0.3 to 3.5. The experiment was carried out at different N_2 percentage, 0-60%. They inferred that the addition of Nitrogen inversely reduced the thermal diffusivity and flame temperature, which consequently slowed down the laminar burning speed. Considering the burning speed as function of fuel-air ratio, the maximum value of the laminar burning speed and the flame instability transition were displaced towards higher equivalence ratio in correspondence with the increase of nitrogen content in the mixture. Agreeable with Prathap et al. conclusion [7], Yepes and Amell results [17] have drawn similar conclusion by decreasing nitrogen content and increasing O_2 from 21% to 35% with 0.8 atmospheric pressure and 298 K. They [17] noted that an increase of 4% O_2, which in turn decrease amount of N_2, results in 25% increase in the burning speed at 0.25 oxidizer-fuel ratio.

For the presence of Carbon dioxide (CO_2) as diluent the burning speed decreases with the increase of the CO_2 concentration in the syngas mixture due decrease in flame

temperature and reaction rate [18-20]. Natarjan et al. [18] examined the CO_2 effect for up to 40% concentration for 5:95, 50:50 and 95:5 H_2:CO mixture with 300K-700K initial temperature and atmospheric pressure using Bunsen burner method. All the three mixtures showed decrease in the burning speed with the dilution of CO_2, however, the increase of mixture temperature indicated rapid increase in the burning speed as the reaction rate and thermal and mass diffusivity increases. Similar conclusion was reached by Minchao Han et al. [19] using constant pressure spherical propagating flame method of 10%-60% H_2, 1%-55% CO, and 5%-70% diluents at 0.1MPa-1MPa pressure and 298K-450K temperature. The increase of CO_2 increases the flame stability even at elevated pressure, while decreases with the increase of temperature and becomes unstable [19]. With different perspective, Jinhua Wang et al. [20] observed the CO_2 effect while increasing the H_2 concentration in the syngas mixture. As the Hydrogen increases the burning speed of syngas as well as the flame cellularity, carbon dioxide inclusion reduces the effect of the hydrogen in the mixture [20].

Tran Manh Vu et al. [21] studied the effect of three diluents namely nitrogen (N_2), helium (He) and carbon dioxide (CO_2) using outwardly expanding flame with constant pressure method for 50:50 H_2:CO ratio at room temperature and 0.1MPa-0.3MPa pressure. The diluents' concentrations were 10% to 30% in the mixture. Comparison of the three diluents illustrated that helium (He) has the least effect on the reduction of laminar burning speed, while CO_2 is being the highest. Also, increasing helium (He) content does not affect the Markstein length whereas N_2 and CO_2 reduce the Markstien length of the mixture [21].

Several other studies were carried out to study the effect of hydrocarbon addition to the syngas mixture such as methane and propane. Lapalme and Seers [22] studied methane addition of 0-40% for 5-95 H_2 ratio at atmospheric pressure, 295-450 K temperatures, and 0.8-2.2 equivalence ratios using Bunsen burner method. Jeong Soo Kim et al. [23] reported a study on counterflow method flame interaction between Methane and 50:50 H_2:CO syngas with 10% CO_2 flames at ambient pressure and temperature with 0.7-4 fuel-air ratios. Tran Manh Vu et al. [24] studied the flame cellularity of 50% H_2 syngas mixture with addition of methane, propane and butane ranging from 5-10 % at ambient temperature, 0.2-0.4 MPa and 0.8-1.2 equivalence ratios. Also, Deepti Signh et al. [25] test syngas burning speed of stoichiometric 1:3 and 1:1 H_2/CO ratio at atmospheric pressure and 400 K with addition of H_2O 0-40% using spherical bomb method. Water moisture increases the burning speed up to 20% concentration then the laminar burning speed is inflected. Whereas Apurba Das et al. [26] indicated that the critical value of moisture addition is at 15% for 5-100% H_2 ratios, 323K and atmospheric pressure and 0.6-0.9 equivalence ratios.

3. Experimental Facilities

In this section the overall experimental setup in the laboratory is described. The individual components are described as well as the experimental procedure that is followed in order to fill the combustion vessels, ignite the mixture, and to collect data.

3.1. Cylindrical Vessel

The laboratory is equipped with 316-stainless steel cylindrical chamber in which the combustion process takes place as shown in figure 1. The inner diameter of the chamber is 13.5 cm with 13 cm long. Both sides of the cylinder have Pyrex windows to allow for optical recording using shadowgraph setup. The windows are 3.5 cm thick and is fitted with silicon O-ring, allowing for a maximum of 50 atmospheres operating pressure. Also, the combustion chamber fitted with a 603BI kistler type pressure transducer that is attached to a charge amplifier of 5010B kistler type to record pressure- time history. For the igniting of the combustible mixture, two axisymmetric spark plugs are installed and extended to provide the required energy for ignition at the center of the chamber. The vessel is designed with provision of 6 mm filling inlet as well as vacuuming outlet at the 6-o'clock position.

3.2. Filling System

The mixture constituents are supplied by pressurized cylinders, which are securely mounted, identified and color-coded per NFPA requirements. The cylinders outlets are equipped with pressure regulators to reduce the gas pressure. Upon the gas pressure reduction, the desired gas passes through a wall-mounted metering station. The metering station consists of three piezoelctric pressure transducers including 15 psia, 30 psia and 50 psia (figure 2). The selection of the pressure transducers is based on the initial

pressure of the filling. The filling process is regulated by a needle type valves installed upstream of the pressure gauges. Also, the metering includes a thermocouple pressure gauge that determines the vacuum in the cylindrical vessel. The whole piping system along with the combustion chamber is connected to a vacuum pump.

3.3. Schlieren/Shadowgraph Assembly

A Z-type shadowgraph setup is assembled with the cylindrical vessel, shown in figure 3, to record a real time motion for the combustible flame propagation. The light supplied from a 10-watts halogen bulb passes through a 0.3 mm hole to elevate its intensity. The light beam travels 152.4 cm with a 15 degrees angle and then gets reflected by a mirror. As the light is reflected, it intersects with the combustion chamber. Consequently, the disturbed light beam is then refocused by another mirror, which directs the light to a high speed CMOS camera. The camera records the combustion flame propagation with a capture rate up to 40,000 frames per second.

3.4. Ignition System

The ignition system consists of an ignition box that provides 5 variation of voltage supply ranging from 20-240 V. In terms of protection to the equipment, the ignition box has optaisolator and isolation transformer to protect against transient current. As the DC pulse transfer to the transformer it supplies 3000 V to the spark plugs (Figure 4). The transformer is a step-up autotransformer (non-separated windings) with 1:100 turn ratio. Consequently, A high voltage potential is created across the spark plugs gap. Therefore once it is broken, a spark is produced inside the chamber providing range from 52 mJ to 420 mJ to ignite the premixed combustible mixture. Figure 5 is a scheme of the ignition circuit.

3.5. Heating System and Temperature Correlation

For the purpose of identifying the combustible mixture's burning speed at above room temperature, the chamber is heated using two heater strips. Each strip is capable of heating up to 500 K. The exposed surface of the cylindrical chamber is well insulated except for the side windows. Two thermocouples of K type are installed at the surface of the cylinder to control the heating cycles of the heater bands through set points programmed in the digital controllers. Each thermocouple is connected to digital DP700X controller.

A correlation was developed to determine the gas temperature inside the chamber based on the chamber's skin temperature identified by the thermocouples. A third thermocouple was placed inside the chamber, while the chamber is at atmospheric pressure. The skin temperatures along with the third thermocouple were registered manually every 30 seconds. The results were plotted, figure 6, in excel program. Roughly a constant difference of 30°C was observed overtime. The correlation was developed for two heating cycles.

3.6. Experimental Procedure

An excel spreadsheet was developed to provide the partial pressure for each syngas component based on the initial pressure and temperature, and equivalence ratio. As the partial pressure is acquired and that the chamber along with the piping system has reached desired vacuum level (below 100 mtorr), the filling starts with the component of the lowest partial pressure and sequentially proceeds with filling the next constituent of higher partial pressure. Between each filling of the mixture's components, the chamber shut-off valve is closed and the piping is vacuumed by the vacuum pump (Welch

Chemstar™1402N). After completing the filling process, the mixture is given 3 minutes prior to the ignition to ensure quiescent state of the mixture.

4. Data Processing

The burning speed calculations are restricted to flames radius greater than approximately 4 cm where the effect of stretch becomes negligible. The camera recording is firstly reviewed to identify the time where the flame reaches the wall of the vessel. A typical pressure file from an experimental run of syngas in the cylindrical vessel is shown in figure 7 with the indication of the cutoff limit identified based on the optical recording. Wrinkles and fluctuation in the pressure curve generate errors upon inclusion in the FORTRAN code. Hence, data smoothing is essential prior to enter it in the code. Depending on the severity of the fluctuation, several smoothing techniques are employed among which is the moving average. Also, the data can be refined using differential slope between points to eliminate negative slopes. However, the physical behavior depicted by the graph must be maintained. That is, the pressure versus time file should represent a monotonically increasing function with time. Also, the flame reaches the vessel wall in the cylinder much earlier than the maximum pressure. In order to determine when the flame hits the vessel's wall, the high-speed camera images are used to find the flame arrival time. There are cases where the flame is completely cellular and were not included in the study. Figure 8 illustrate a case where cellularity develops at very early stage of the flame. Only smooth flames are considered in the data analysis.

5. Uncertainty of Results

An uncertainty exist in this study is due to couple of factors. Converting the molar fraction of the mixture's components to be measured by the pressure transducer, generates an error of around 1%. In addition, the filling procedure may induce further error of roughly 0.5%. Furthermore, the error that results from heating the mixture may account for about 1%. As the result of the pressure history data must be smoothed, this process may develop an error ranging from 1% to 4%. With the consideration of all the above factors, the total error would range from 3.5% to 6.5%.

6. Thermodynamic Model

To calculate the laminar burning speed in this study, a model originally developed by Metghalchi and Keck [27] was used. Laminar burning speed is calculated using the experimental pressure rise history during the propagation of the flame inside the sphere. To simplify the complexity of the burning speed phenomena, critical assumptions were employed in this model. The gases inside the spherical chamber occupy two distinguished regions that are burned and unburned zones. The reaction occurs between those two zones and occupies negligible thickness. Although the pressure increases during the process, it uniformly increases inside the chamber. Both the burned and unburned gases assumed to behave as ideal gases and they are compressed isentropically. Later, the model was adjusted to accommodate the losses of energy to the vessel wall and electrode. In addition, the model accounted for the energy transfer by heat radiation and considered the gradient of temperature inside the preheat zone.

As shown in figure 9, the burned gas zone at which the ignition source is centrally located is partitioned into small shells. The number of shells is proportional to the duration of combustion. Although the temperature is deferent in each shell, they are considered in chemical equilibrium. STANJAN has been used to calculate burned gas properties considering species listed in table 1. The burned zone bounded by a variable temperature preheat zone (δ_{ph}) followed by the unburned region. Two thermal boundary layers are considered in this model, a thermal boundary layer between the unburned zone and the chamber wall (δ_{wb}) and the other thermal boundary layer accounts for the heat interaction between the burned zone and the electrode (δ_{bl}).

Since the gas is assumed to depict ideal gas behavior, the system is governed by three equations that are ideal gas equation of state, continuity equation and energy conservation. The following equations are solved simultaneously:

$$Pv = RT \tag{1}$$

Where P is the pressure, v is the specific volume, R is the specific gas constant and T is the temperature. The mass conservation equation for the burned and unburned gas regions is:

$$m = m_b + m_u = P_i(V_c - V_e)/RT_i \tag{2}$$

m : Total mass of the chamber,

m_b : Mass of the burned gas zone

m_u : Mass of the unburned gas zone

V_c : Volume of the chamber and

V_e : Volume of the spark electrodes

Where i refers to the initial conditions, *u* and *b* denote the unburned and burned gas conditions.

The total volume of the gas in the combustion chamber is:

$$V_i = V_c - V_e = V_b + V_u \tag{3}$$

and the energy conservation equation is:

$$E_i - Q_e - Q_w - Q_r = E_b + E_u \tag{4}$$

E_i : initial energy of the gas

Q_e : conductive energy loss to the electrodes,

Q_w : energy loss to the wall,

Q_r : radiation energy loss.

Volume derived from mass balance and energy balance equations can be written as:

$$\int_0^{x_b}(v_{bs} - v_{us})dx = v_i - v_{us} + (V_{eb} + V_{wb} + V_{ph})/m \tag{5}$$

$$\int_0^{x_b}(e_{bs} - e_{us})dx = e_i - e_{us} + (\frac{pV_{ph}}{\gamma_b - 1} + \frac{pV_{eb}}{\gamma_b - 1} + \frac{pV_{wb}}{\gamma_b - 1} - Q_r)/m \tag{6}$$

where,

$v_i = (V_c - V_e)/m$ is the initial specific volume

$e_i = E_i/m$ is the energy of the unburned gas

v_{bs} : Specific volume of isentropically compressed burned gas,

v_{us} : Specific volume of isentropically compressed unburned gas.

V_{wb} : Displacement volume of wall boundary layer

V_{ph} : Displacement volume of preheat zone ahead of the reaction layer

V_{eb} : Displacement volume of electrode boundary layer

e_{bs} : Specific energy of isentropically compressed burned gas

e_{us} : Specific energy of isentropically compressed unburned gas

γ_u : Specific heat ratio of unburned gas

These equations are invoked to solve for the burned gas mass fraction and the burned gas temperature of the last shell. Consequently and identifying experimentally the pressure as a function of time, they can be solved numerically to find the burned mass fraction $x_b(t)$ and radial temperature distribution $T(r,t)$. Hence, the laminar burning speed can be identified through the following equation:

$$S_u = \dot{m}_b / \rho_u A_b = m\dot{x}_b / \rho_u A_b \tag{7}$$

Where A_b is the area of the sphere having a volume equal to that of the burned gas.

7. Results

7.1. Flame Structure

The measurement of the laminar burning speed in this study is considered for smooth flame structure. Hence, the optical recording was used to ensure the inclusion of only smooth flame structure's pressure data. Figure 10 shows a case of initial condition of 380K, 1 atm and equivalence ratio of 3. The cut off limit for the data was at frame 63(21 ms), just before the flame hit the wall. Another case is shown in figure 11 for 380K, 2 atm and equivalence ratio of 3 where the measurement of laminar burning speed was excluded due to the cellularity development before the flame radius reaches 4cm. Also, comparing figure 10 and 11, it can be induced that the increase of initial pressure causes the cellularity to develop at earlier stage.

7.2. Flame Stretch

It is crucial to evaluate the stretch effect on the laminar burning speed to validate the obtained laminar burning speed values. Flame stretch is caused by the variation of flame area over time. For spherically expanding flames stretch rate can be defined as:

$$\kappa = \frac{1}{A}\frac{dA}{dt} = \frac{2}{r}\frac{dr}{dt} \tag{9}$$

Where κ is the stretch rate, A is the area of flame, t is time, and r is the flame radius.

The effect of stretch on the laminar burning speed was studied for different initial conditions, which are 298, 350 and 380K along with pressures that corresponds to the isentropic curve. Two cases were considered pertinent to 0.6 and 3 equivalence ratio.

These conditions were selected in such a way that they have different radii so that the laminar burning speed can be evaluated at different stretch rates. Figures 12 shows variation of burning speed along stretch rate for 0.6 equivalence ratio for temperature of 390 K and pressure 1.294 atm. Also, figure 13 shows variation of laminar burning speed versus stretch rates for 3 equivalence ratios for temperature 400 K and pressure 1.359 atm. From the figures, variation of laminar burning speeds in this range of stretch rate is negligible since the burning speed maintain constant line over the values of the stretch rate. Therefore all our data collected for flame radius greater than 4 cm is not affected by the flame stretch.

7.3. Laminar Burning Speed

Laminar burning speed has been studied for syngas with 5% H_2 and 95% CO for the range of 0.6 to 5 equivalence ratios, pressure ranging from 0.5 atm to a maximum of 3.2 atm and temperatures ranging from 315 K and 490 K. It is clear from the optical recording that the increase of pressure inversely affects the burning speed of the mixture. Figure 14 illustrates the expansion of the flame radius over time for 298 K initial temperature, 0.6 equivalence ratio and with range of 0.5 atm to 2 atm initial pressures. Figure 15 shows the laminar burning speed of syngas along an isentrope for initial temperature of 298K and 0.5 pressure with equivalence ratios ranging from 0.6 to 5. Clearly, there is a rapid increase in the burning speed as the equivalence ratio increase from lean mixture of 0.6 ratio to reach mixture up until 3.0 air-fuel ratio. The burning speed reaches its peak at 3.0 equivalence ratio and then decreases as indicated by the results of 5.0 air-fuel ratio. Figure 16 and 17 for 298K initial temperature, 1atm and 2 atm initial pressures respectively and equivalence ratios from 0.6 to 5 illustrate similar trend

for the burning speed. However, the laminar burning speed decreases with the increase of the initial pressure. Also, figure 18 illustrate the trend of laminar burning speed along isentrope curve for initial conditions at 380K, 0.5 atm over the range of 0.6 to 5 equivalence ratios. By comparing figure 15 and 18, the laminar burning speed increases as the initial temperature increases. For the same initial temperature of 380K, figure 19 illustrate the laminar burning speed for initial pressures of 1atm and equivalence ratio ranging from 0.6 to 5. It is noteworthy that even at higher temperature (380K), the laminar burning speed depict similar trend to 298K initial condition with the variation of equivalence ratios. However, for 2 atm and 380K conditions, shown in figure 20, the only measurements included are for equivalence ratio of 0.6 and 1 since cellularity develops very early at higher equivalence ratios.

Figure 21 shows comparison between present work and available data in the literature for ambient temperature and pressure. The results shows very good agreement with other results, except for equivalence ratio of 0.6 and 3. Also, the burning speed trend of this study over the test range of equivalence ratios agrees with other researchers' results as the peak is reached at equivalence ratio of 3.

8. Summary and Conclusion

Laminar burning speed has been measured for syngas with 5% H_2 and 95% CO mixture. The study was covered for initial conditions of 298K and 380K temperatures and pressures from 0.5 atm to 2 atm with a wide range of equivalence ratio ranging from 0.6 to 5. Pressure rise history data of an outwardly expanding flame at constant volume was used to calculate the burning speed. The laminar burning speed was calculated over the range of temperature between 315 K to 490 K and range of pressure between 0.6 atm to 3.2 atm. Laminar burning speed changes with fuel air equivalence ratio showing maximum value at equivalence ratio of 3. In addition, laminar burning speed was found to decrease with the increase of initial pressure and increased with the increase of initial temperature. Also, cellularity develops at early stage as the initial pressure increases. Moreover, Comparison of measured burning speed with those of available data in literature is very good.

REFERENCES

[1] Glassman, Irvin, Combustion. 3rd ed. United States: Academic Press, 1996.

[2] Metghalchi, Hameed M., PhD Thesis (1980), Massachusetts Institute of Technology.

[3] Rallis, C. J., Garforth, A. M., "The determination of laminar burning velocity." Prog. Energy Combustion 6 (1980): 303-329

[4] kurucz, Adorjan, Bencik, Izsak, Syngas: Production Methods, Post Treatment and Economics. New York: Nova Science Publishers Inc., 2009.

[5] Puigjaner, Luis, Syngas from Waste. New York: Springer, 2011.

[5] F. N. Egolfopoulos, D. L. Zhu and C. K. Law, Proceeding of Combustion Institute (1991) 471-478.

[6] Zhang, Yang et al. "Laminar flame speed studies of lean premixed H2/CO/air flames." Combustion and Flame 161 (2014): 2492-95.

[7] Prathap, C. et al. "Investigation of nitrogen dilution effects on the laminar burning velocity and flame stability of syngas fuel at atmospheric condition." Combustion and Flame 155 (2008): 145-160.

[8] Bouvet, N et al. "Flame Speed Characteristics of Syngas (H_2-CO) with Straight Burners for Laminar Premixed Flames." Proceedings of the European Combustion Meeting (2007).

[9] Bouvet, N et al. "Characterization of syngas laminar flames using the Bunsen burner configuration." International Journal of Hydrogen Energy 36 (2011): 922-1005.

[10] H. Sun, H. et al., Proceeding of Combustion Institute 31 (2007) 439-446.

[11] J. Li, J. et al., Int. J. Chemical Kinetics 39 (2007) 109-136.

[12] R. Sivaramakrishnan, R. et al., Proceeding of Combustion Institute 31 (2007) 429-437

[13] S.G. Davis et al., Proceeding of Combustion Institute 30 (2005) 1283-1292.

[14] Bouvet, Nicolas et al. "Experimental studies of the fundamental flame speeds of syngas (H2/CO)/air mixtures." Proceedings of the Combustion Institute 33 (2011): 913-20.

[15] Dong, Chen et al. "Experimental study on the laminar flame speed of hydrogen/carbon monoxide/air mixtures." Fuel 88 (2009): 1858-63.

[16] Liu, C C et al. "Hydrogen/carbon monoxide syngas burning rates measurements in high-pressure quiescent and turbulent environment." International Journal of Hydrogen Energy 36 (2011): 8595-603.

[17] Yepes, Hernando A. et al., "Laminar burning velocity with oxygen-enriched air of syngas produced from biomass gasification." International Journal of Hydrogen Energy 38 (2013): 7519-7527.

[18] Narajan, J. et al., "Laminar flame speeds fo H_2/CO mixtures: Effects of CO_2 dilution, preheat temperature, and pressure." Combustion and Flame 151 (2007): 104-119.

[19] Han, Minchao et al., "Laminar flame speeds of H_2/CO with CO_2 dilution at normal and elevated pressures and temperatures." Fuel 148 (2015): 32-38.

[20] Wang, Jinhua et al., "Laminar burning velocities and flame characteristics for CO-H_2-CO_2-O_2 mixtures." International Journal of Hydrogen Energy 37 (2012): 19158-19167.

[21] Vu, Tran Manh et al., “Effects of diluents on cellular instability on outwardly propagating spherical; syngas-air premixed flames.” International Journal of Hydrogen Energy 35 (2010): 3868-3880.

[22] Denis Lapalme, Patrice Seers, “Influence of CO_2, CH_4, and initial temperature on H_2/CO laminar flame speed.” International Journal of Hydrogen Energy 39 (2014): 3477-3486.

[23] Kim, Jeong Soo et al., “A study on methane-air premixed flames interacting with syngas-air premixed flames.” International Journal of Hydrogen Energy 35 (2010): 1390-1400.

[24] Vu, Tran Manh et al., “Effects of hydrogen addition on cellular instabilities in expanding syngas-air spherical premixed flames.” International Journal of Hydrogen Energy 34 (2009): 6961-6969.

[25] Singh, Deepti et al., “An experimental and kintetic study of syngas/air combustion at elevated temperature and the effect of water addition.” Fuel 94 (2012): 448-456.

[26] Das, Apurba K. et al., “Laminar flame speeds of moist syngas mixtures.” Combustion and Flame 158 (2011): 345-353.

[27] M. Metghalchi, J.C. Keck, *Combust Flame* 38 (1980) 143–154.

[28] Hassan M. I. et al., “Properties of laminar premixed CO/H_2/air flames at various pressures.” Journal of Propulsion and Power 13 (1997): 239-245.

[29] Mclean I. C. et al., Proceeding of Combustion Institute 25 (1994): 749-757.

TABLES

Table 1: List of species present in equilibrium used in STANJAN calculations.

H_2	H	O	O_2	OH	H_2O	H_2O_2	C
CH	CH_2	$CH_2(S)$	CH_3	CH_3	CO	CO_2	HCO
CH_2O	CH_2OH	CH_3O	CH_3OH	C_2H	C_2H_2	C_2H_3	C_2H_4
HCCO	CH_2CO	HCCOH	CH_3CHO	CH_3CHO	N_2		

FIGURES

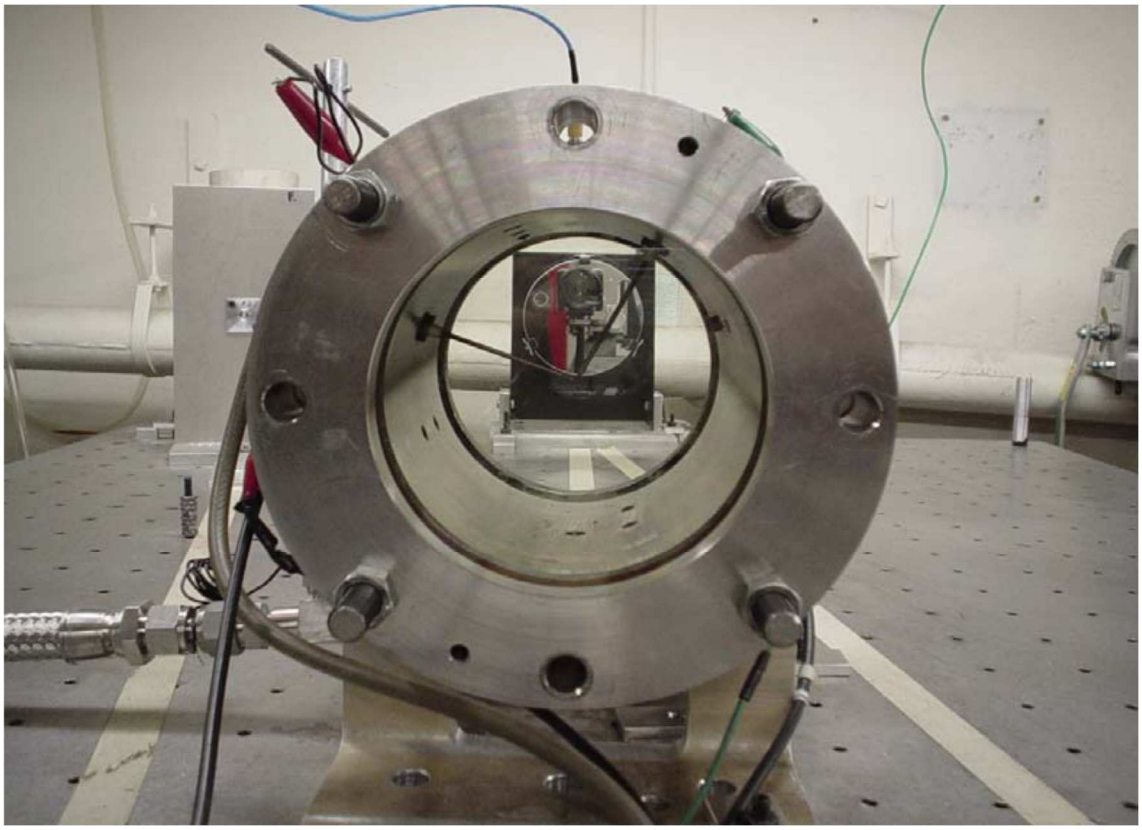

Figure 1: Cylindrical combustion chamber

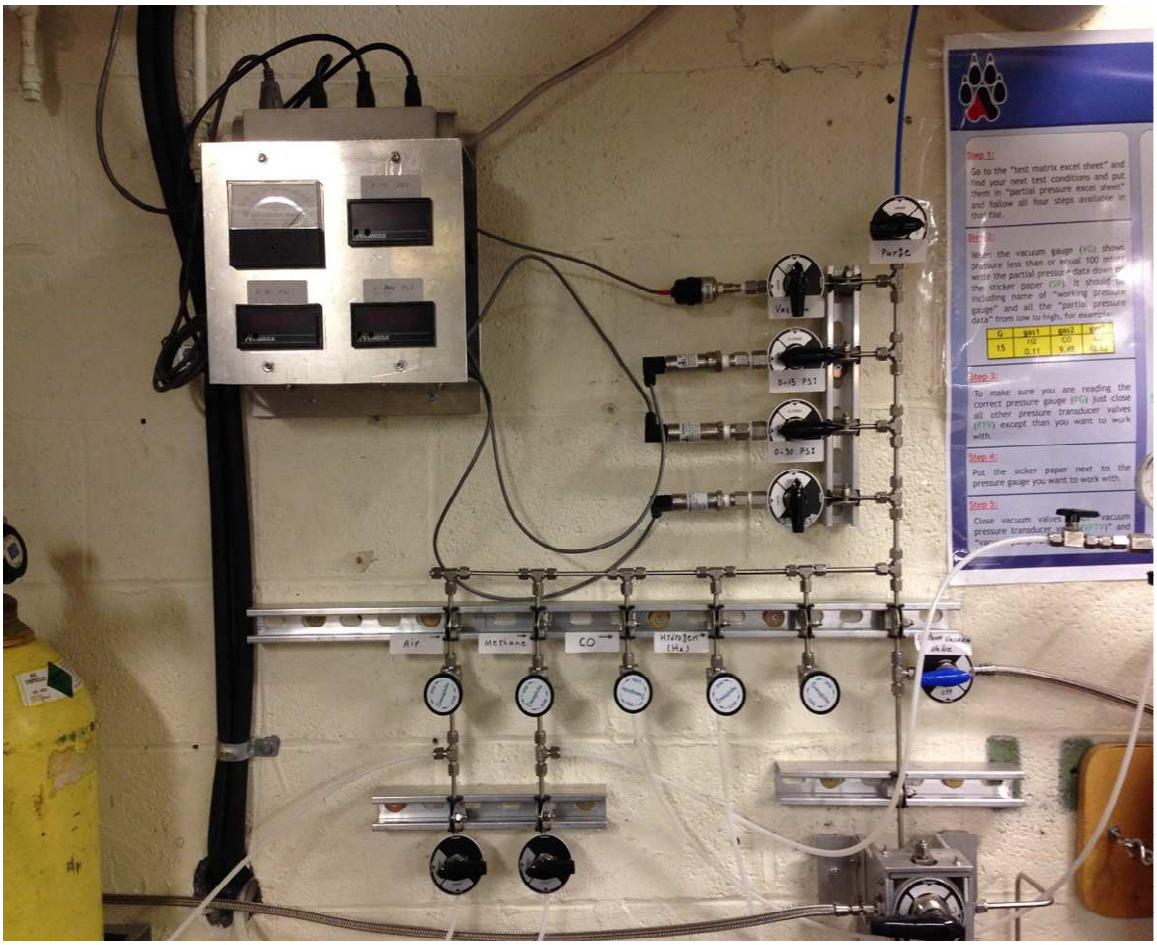

Figure 2: Metering and pressure gauges

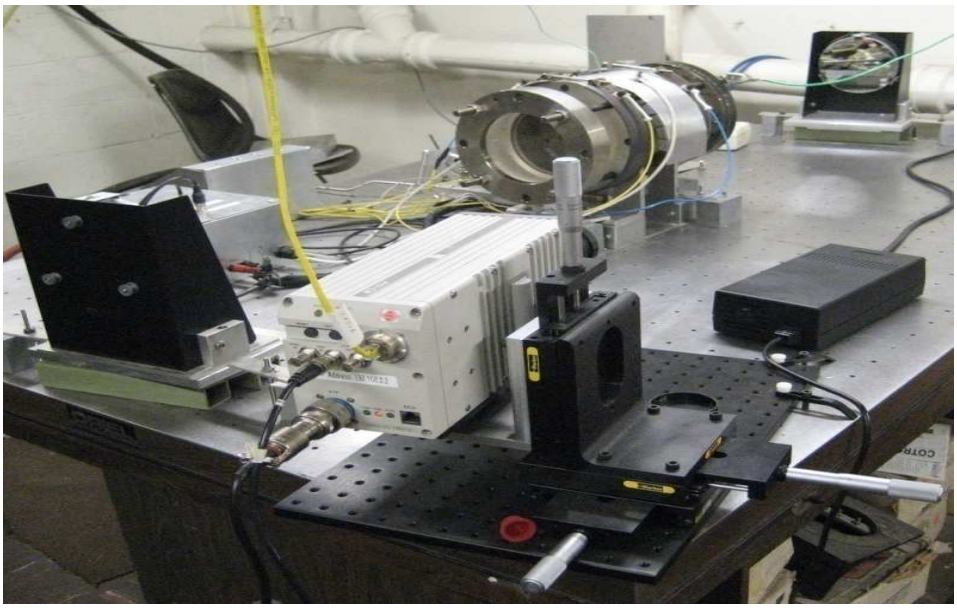

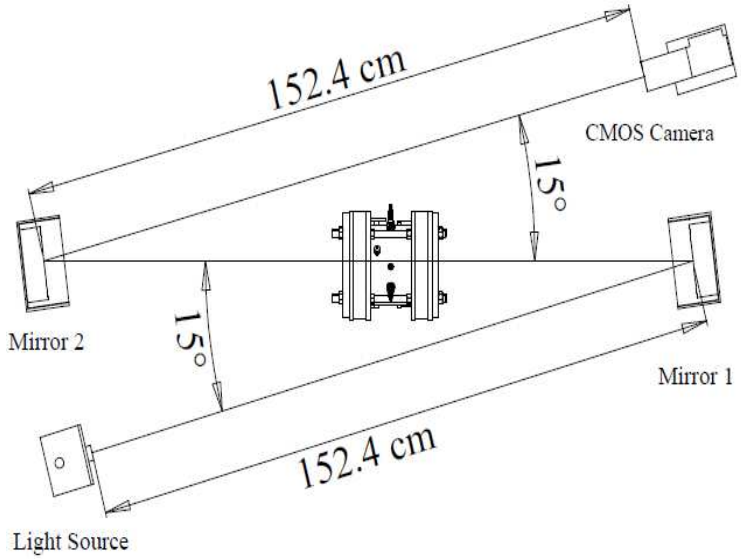

Figure 3: Z-type Schlieren/Shadowgraph ensemble with a high speed CMOS camera.

Figure 4: Typical automotive spark plugs modified with extended electrode for use in combustion vessels.

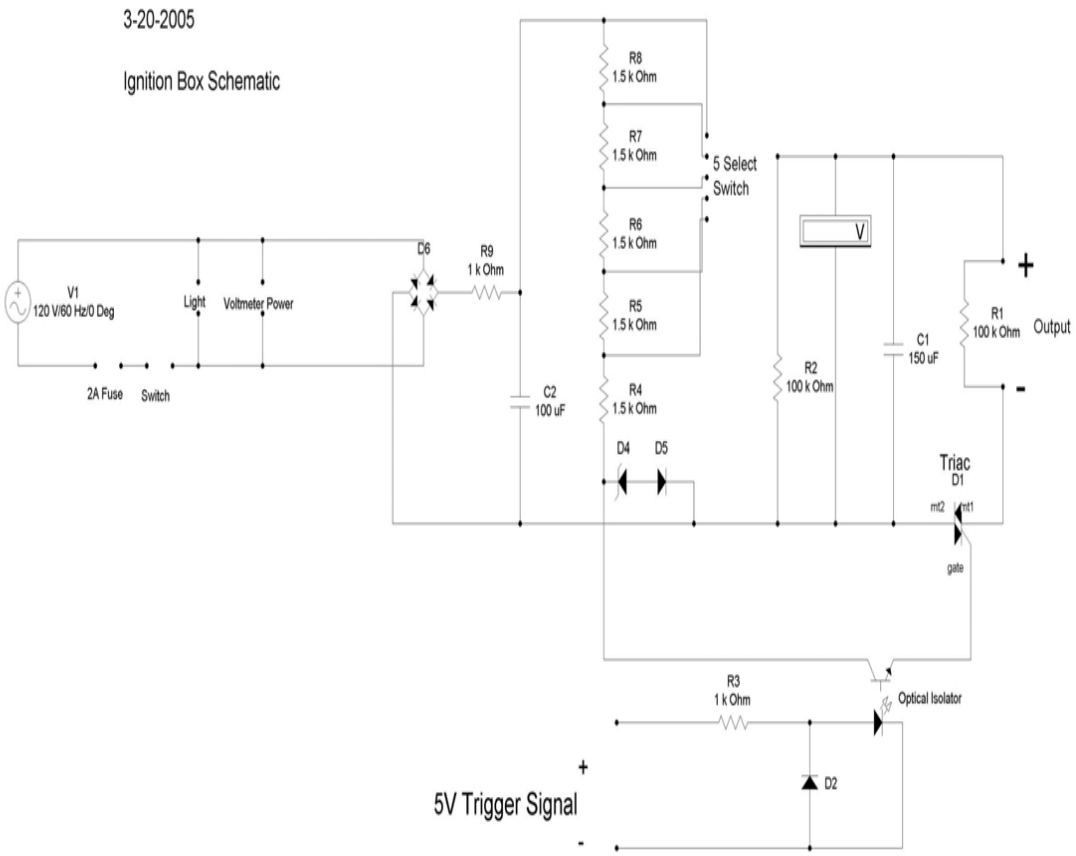

Figure 5: Schematic of ignition circuit.

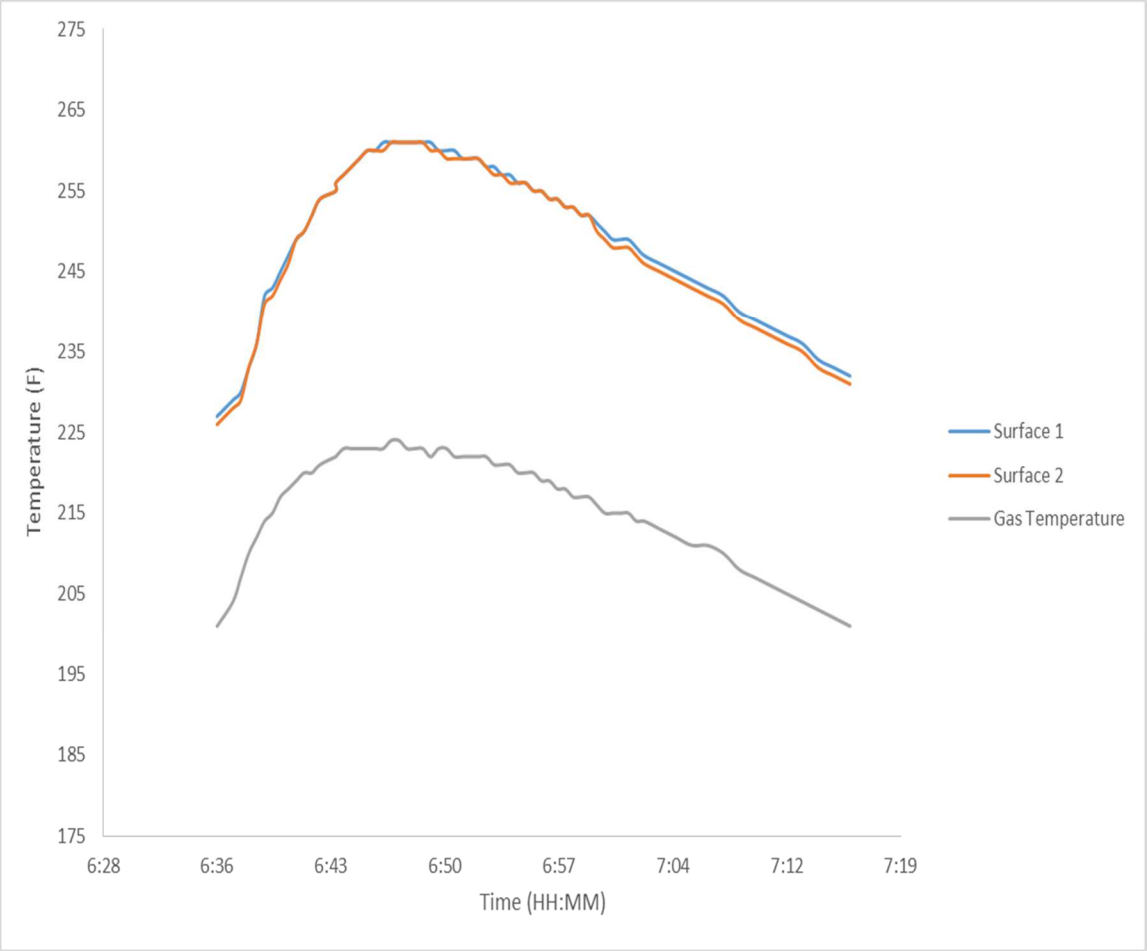

Figure 6: Temperature correlation between the cylinder surface and gas temperature at atmospheric conditions.

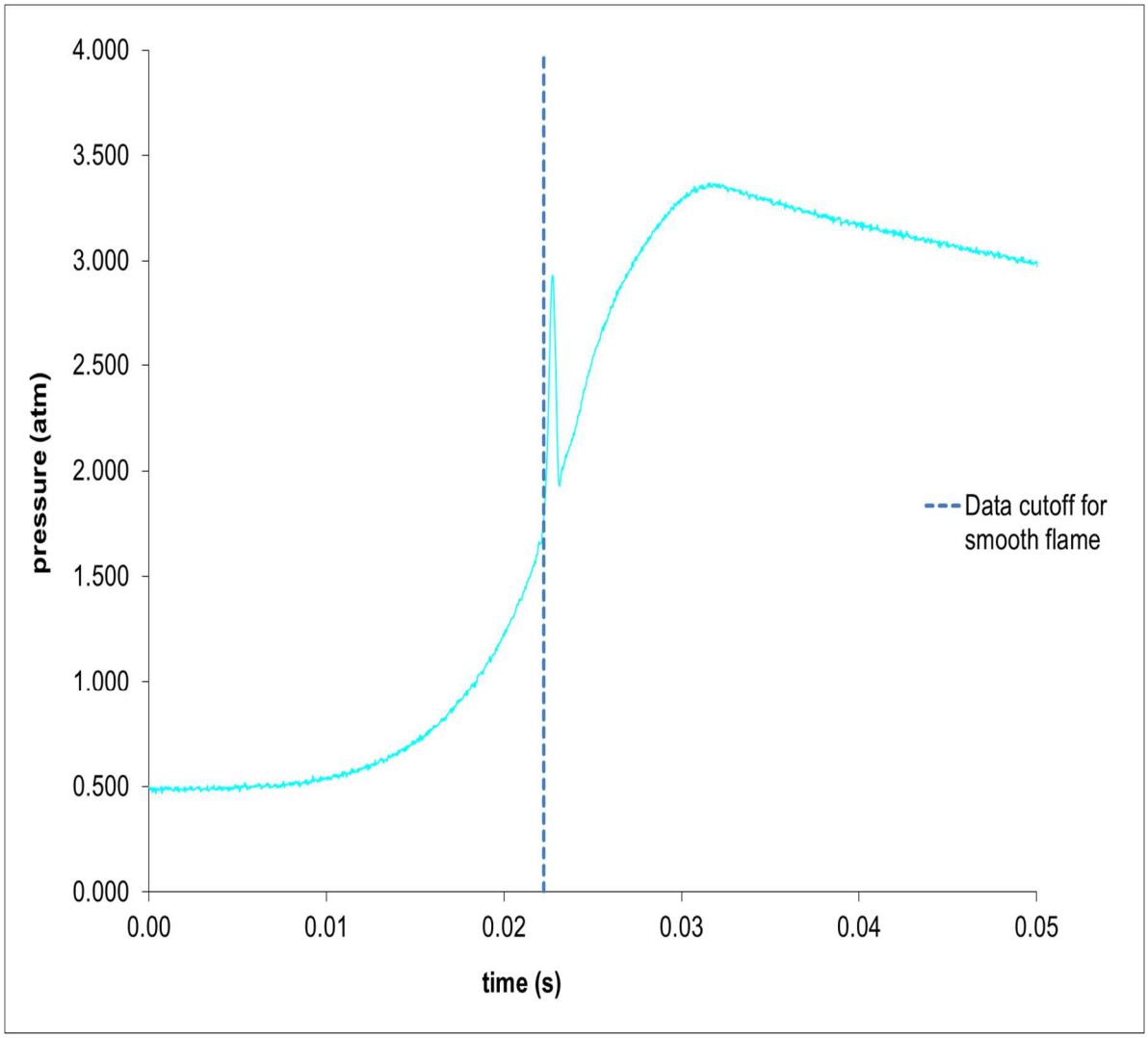

Figure 7: Sample pressure data for initial temperature 298K, initial pressure 0.5 atm and equivalence ratio Φ=3.

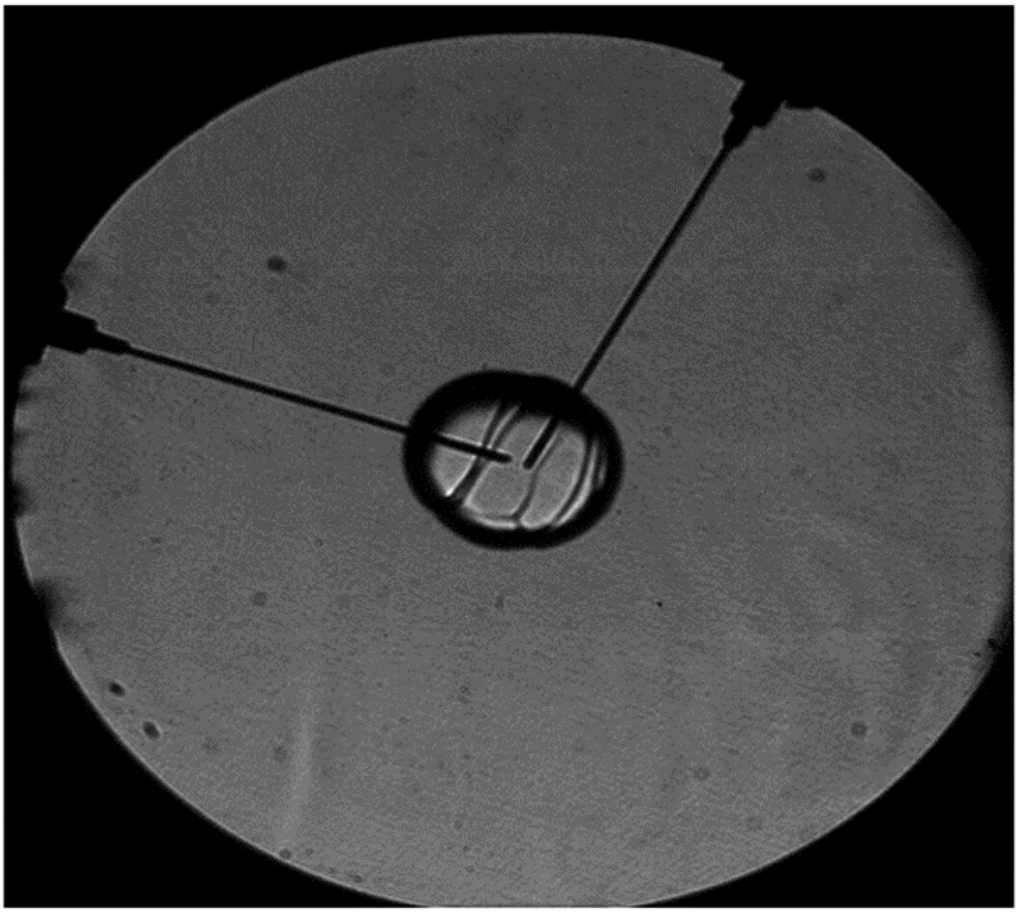

Figure 8: Cellularity develops at early stage of the flame for initial temperature 380K, initial pressure 2atm, and equivalence ratio Φ=3.

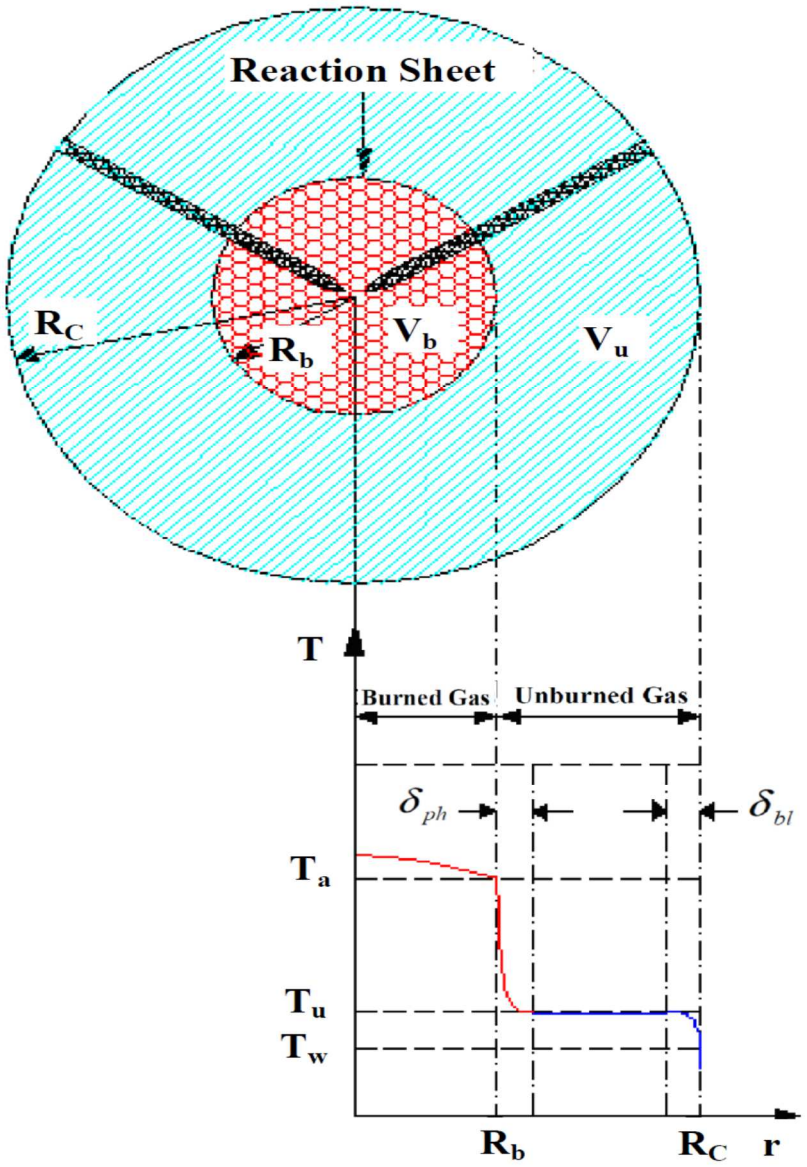

Figure 9: Schematic of different zones and their corresponding temperatures in the thermodynamics model.

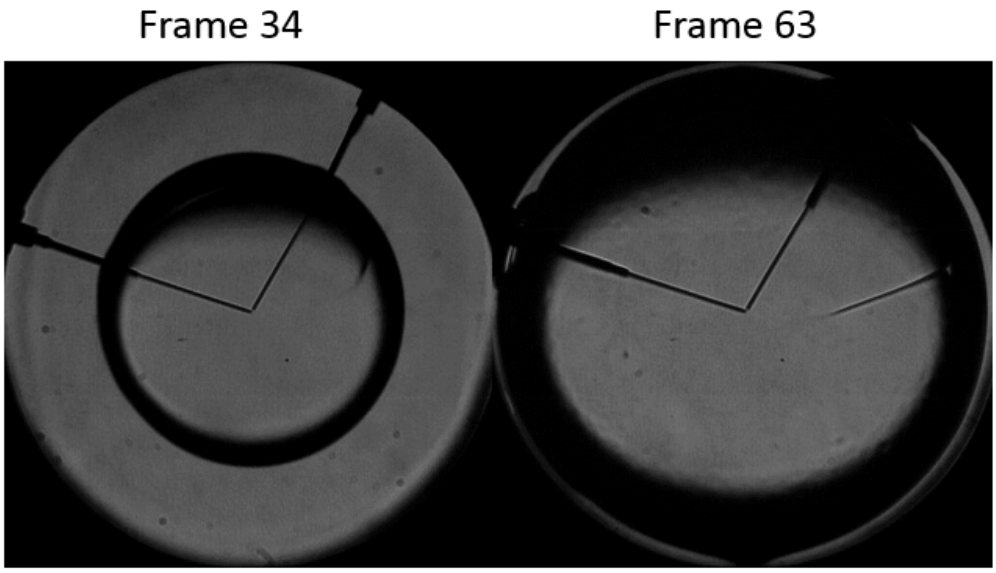

Figure 10: Cellularity development for initial temperature of 380 K, initial pressure of 1 atm and equivalence ratio of 3.

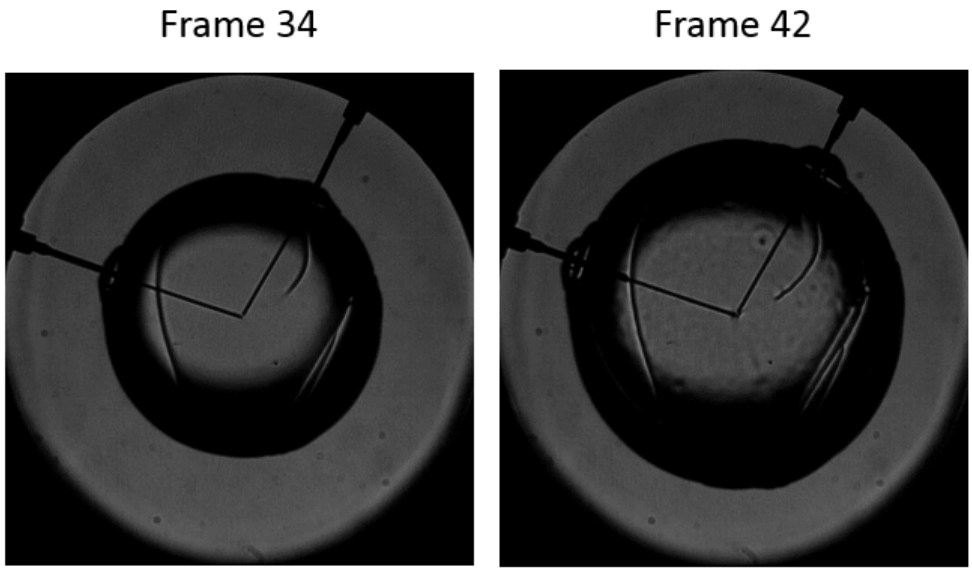

Figure 11: Cellularity development for initial temperature of 380 K, initial pressure of 2 atm and equivalence ratio of 3.

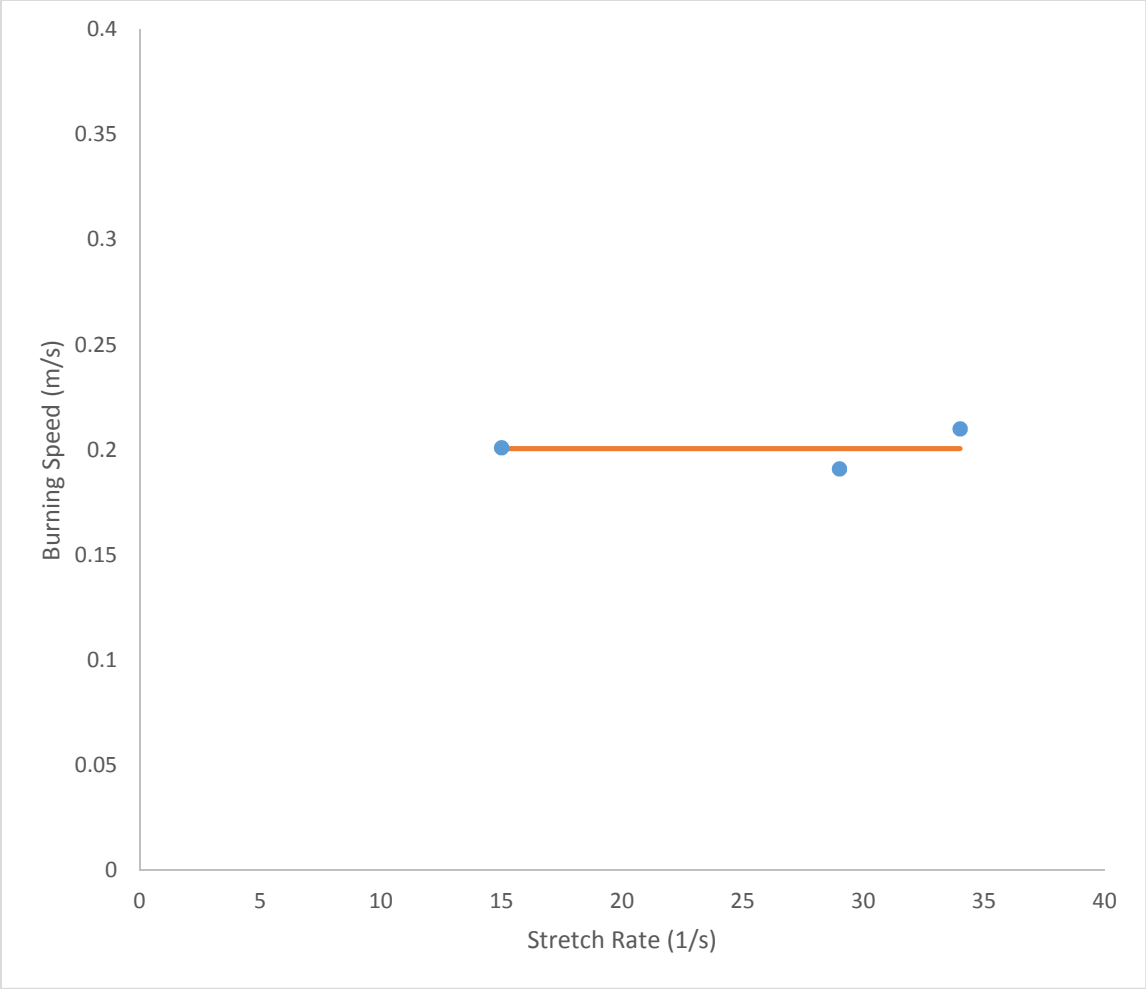

Figure 12: Burning speed verses stretch rate for 0.6 equivalence ratio, T_i= 390 K and P_i=1.294 atm.

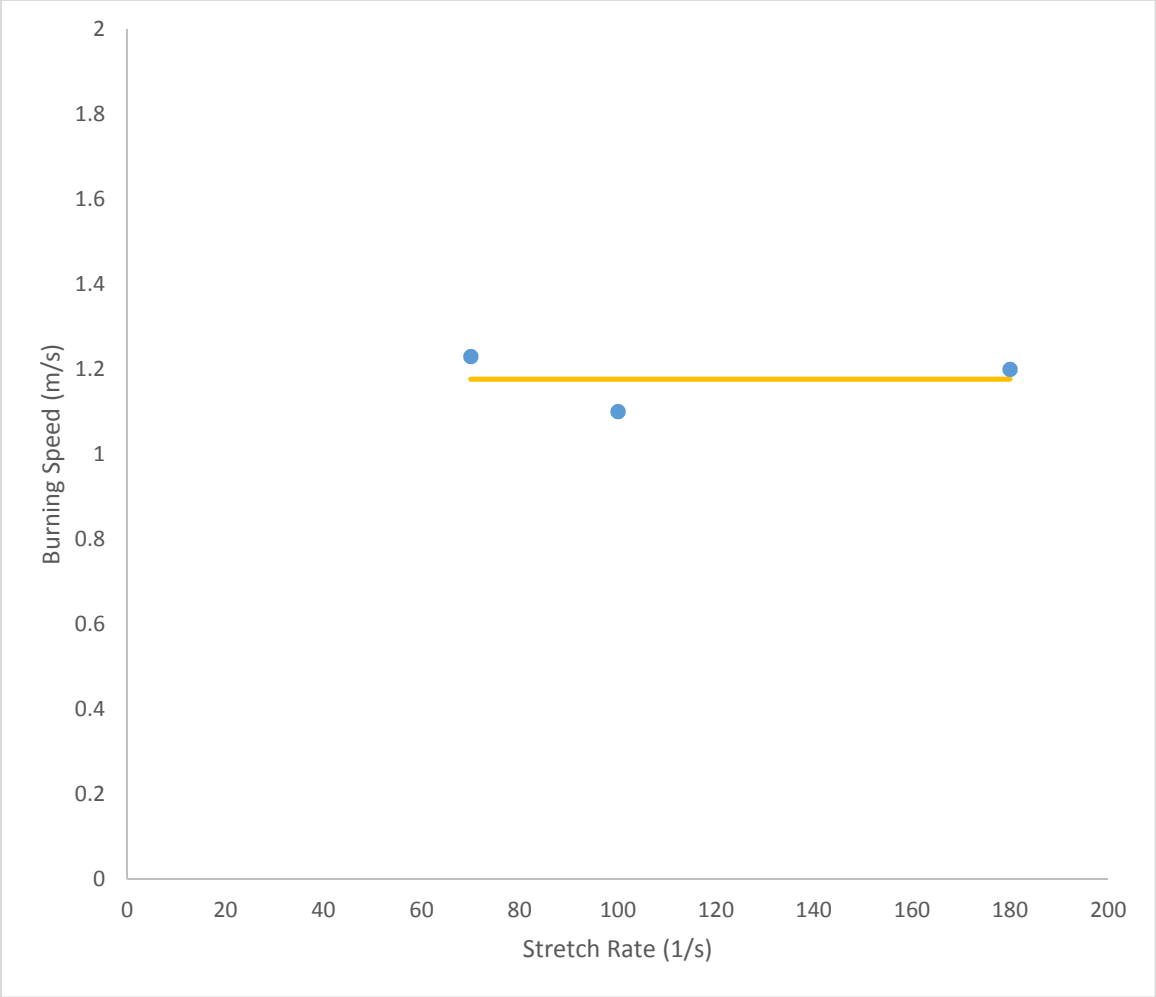

Figure 13: Burning speed verses stretch rate for 3 equivalence ratio, T_i=400 K and P_i=1.359 atm.

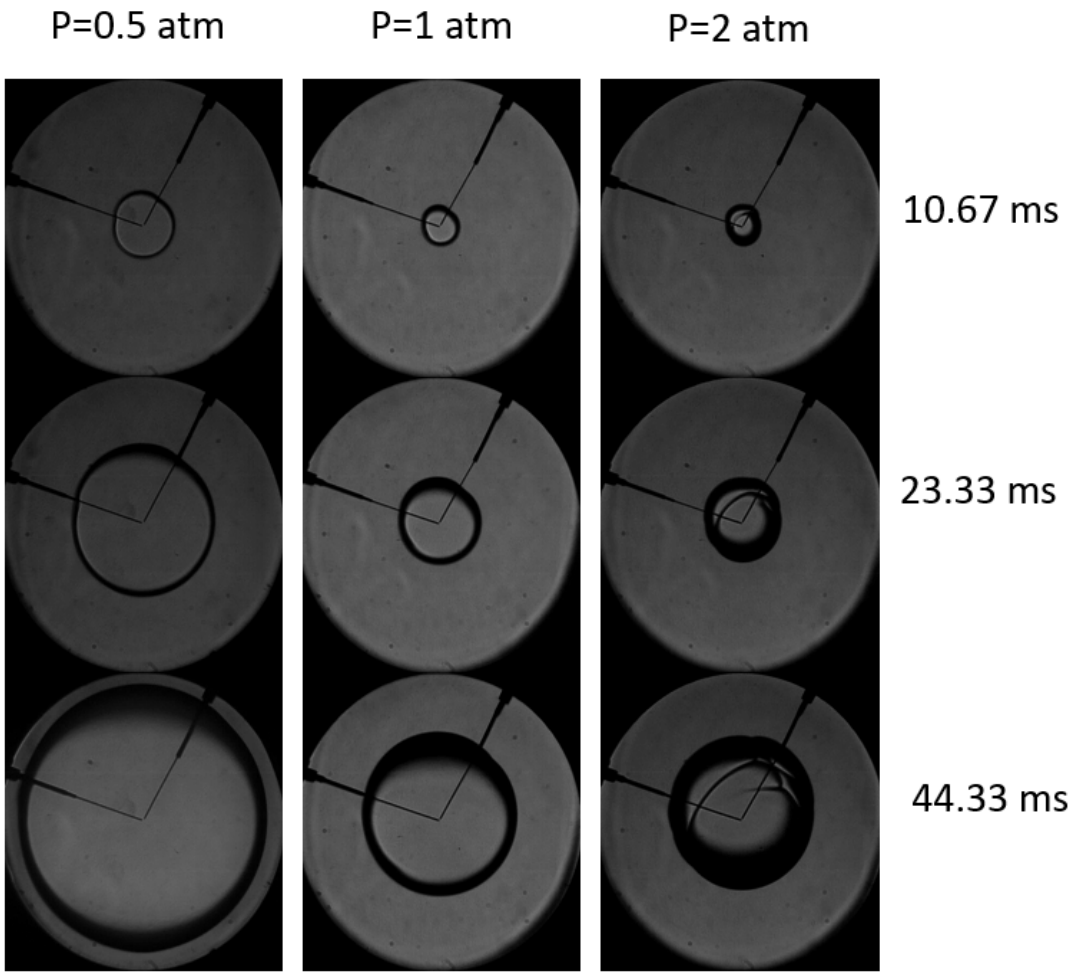

Figure 14: Comparison of flame expansion from 0.5 atm to 2 atm initial pressure, 298K initial temperature and 0.6 equivalence ratio.

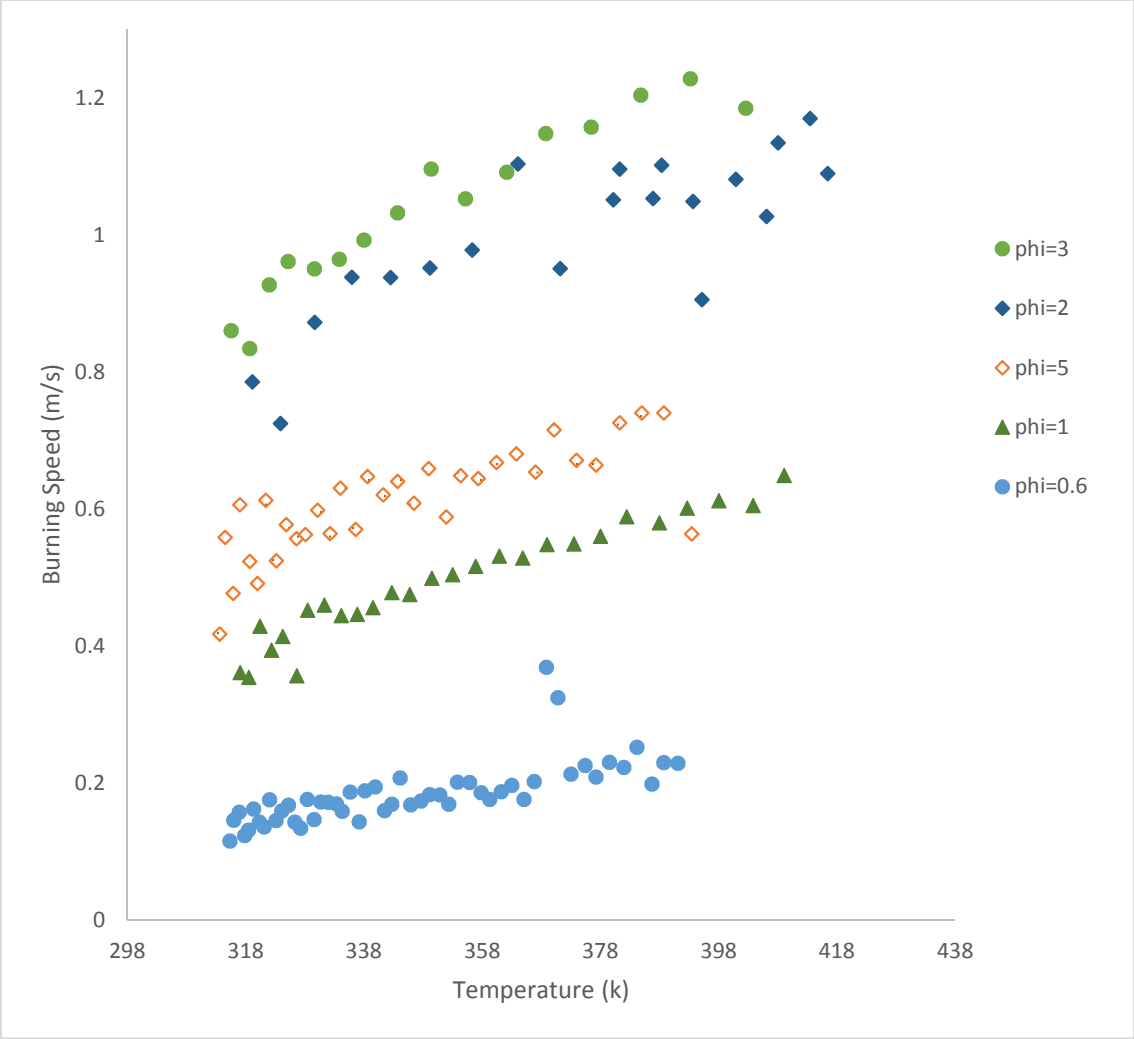

Figure 15: Laminar burning speeds of syngas/air mixture along an isentrope with initial temperature of 298 K, initial pressure of 0.5 atm and fuel air equivalence ratio ranging from 0.6 to 5.

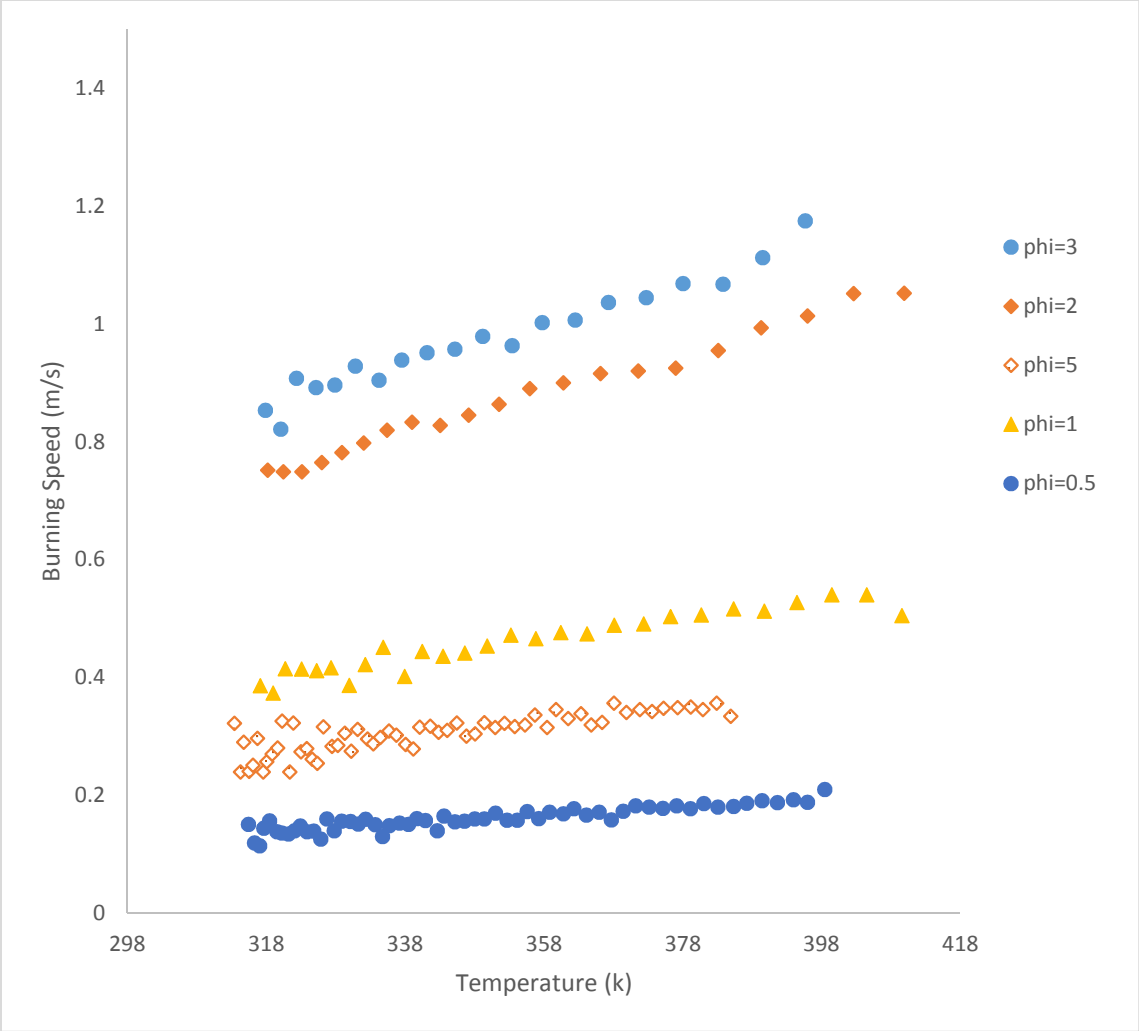

Figure 16: Laminar burning speeds of syngas/air mixture along an isentrope with initial temperature of 298 K, initial pressure of 1.0 atm and fuel air equivalence ratio ranging from 0.6 to 5.

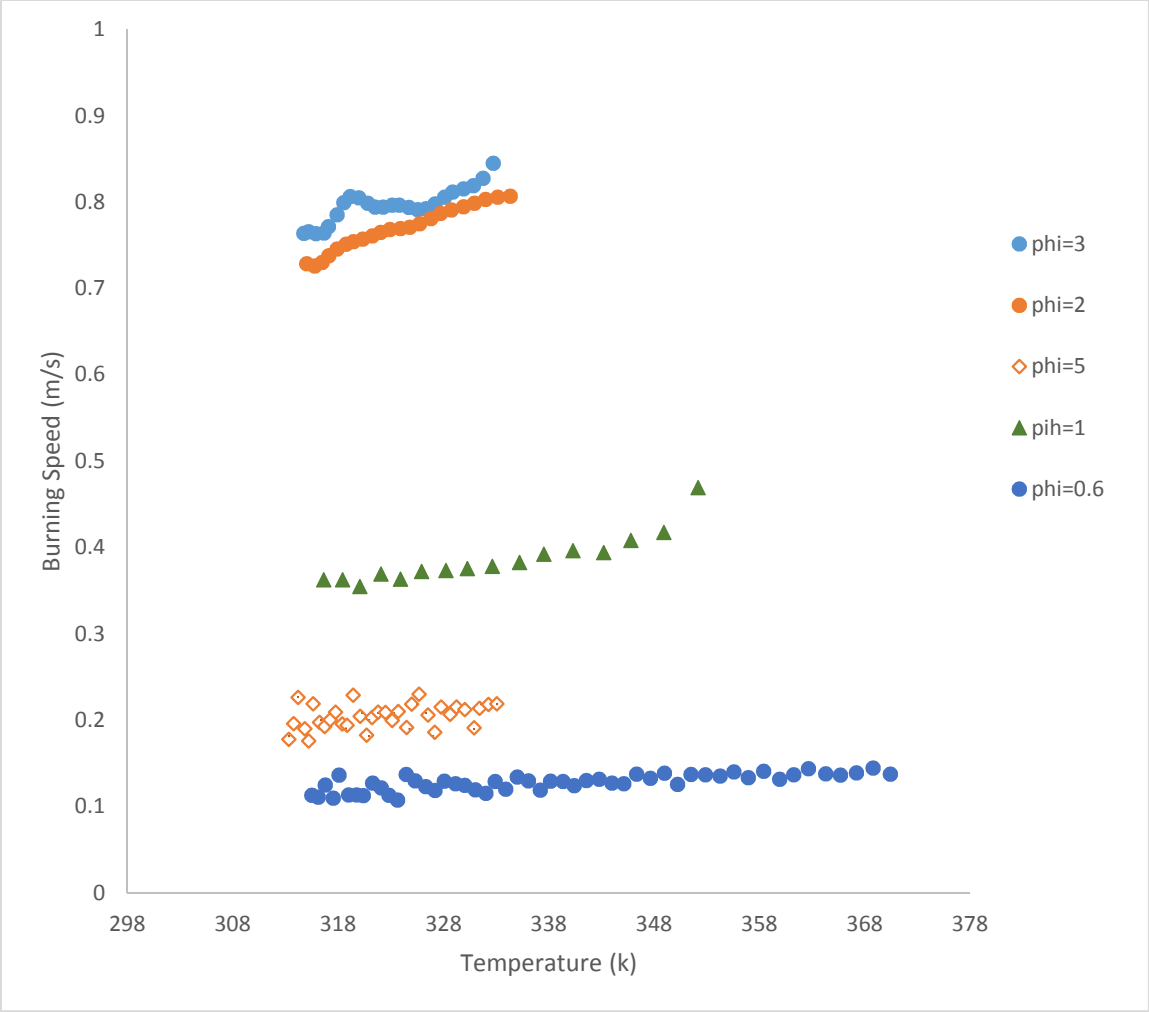

Figure 17: Laminar burning speeds of syngas/air mixture along an isentrope with initial temperature of 298 K, initial pressure of 2.0 atm and fuel air equivalence ratio ranging from 0.6 to 5.

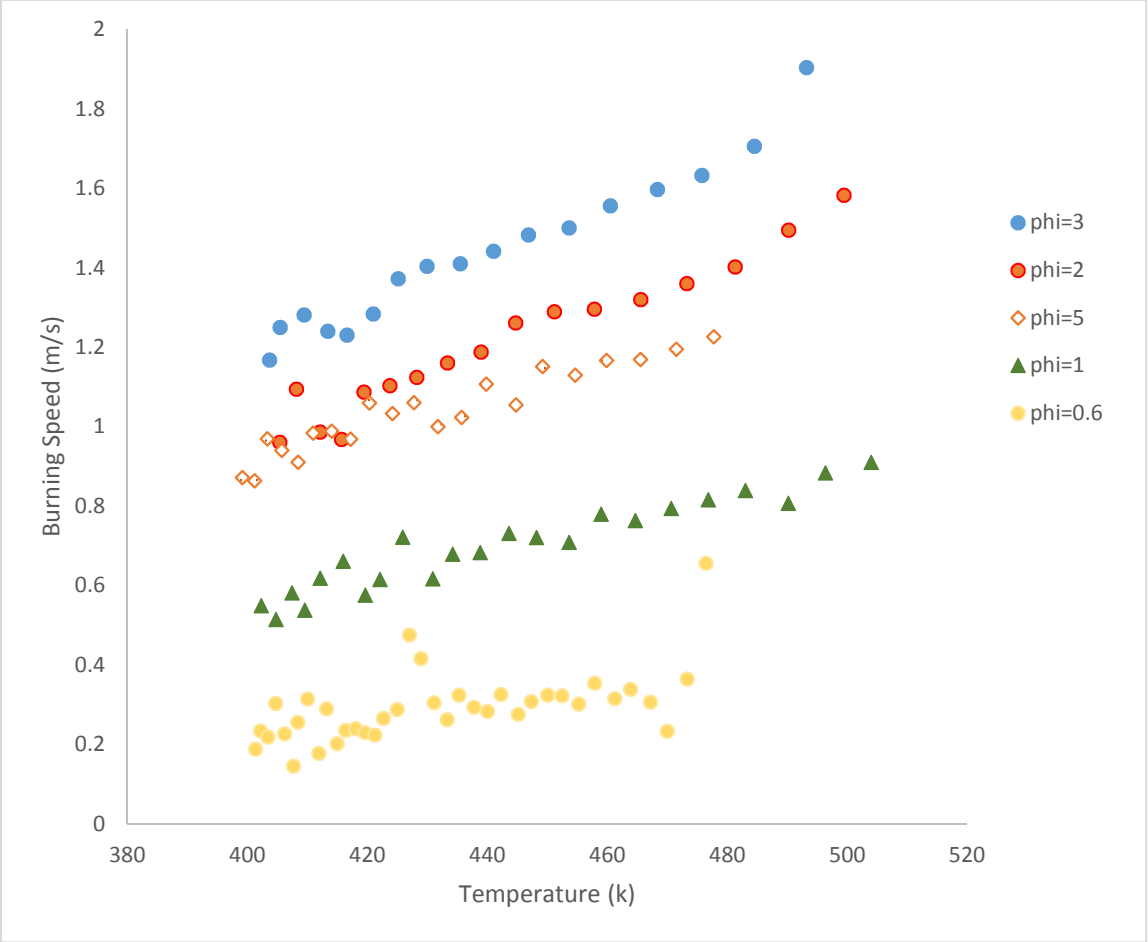

Figure 18: Laminar burning speeds of syngas/air mixture along an isentrope with initial temperature of 380 K, initial pressure of 0.5 atm and fuel air equivalence ratio ranging from 0.6 to 5.

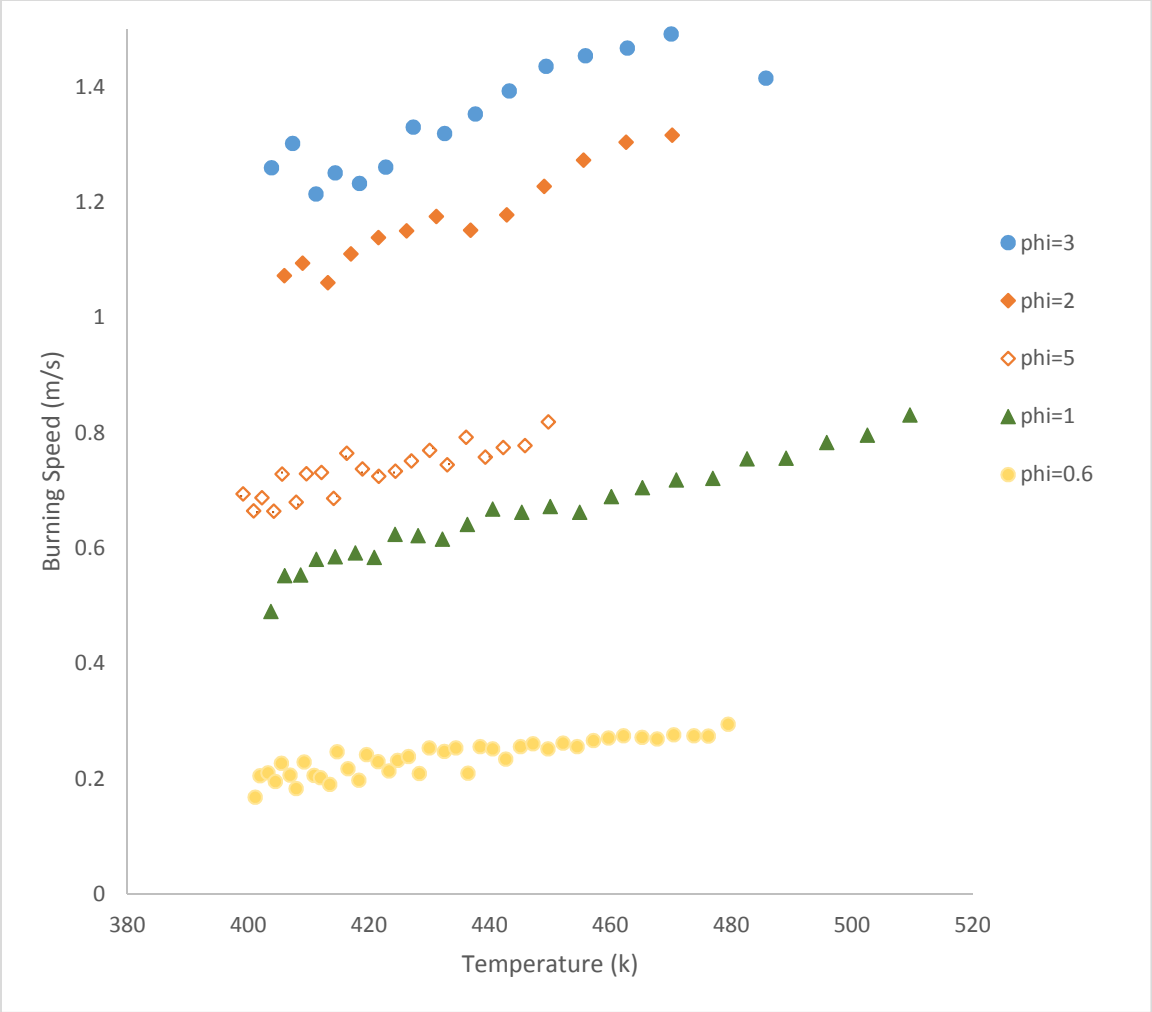

Figure 19: Laminar burning speeds of syngas/air mixture along an isentrope with initial temperature of 380 K, initial pressure of 1.0 atm and fuel air equivalence ratio ranging from 0.6 to 5.

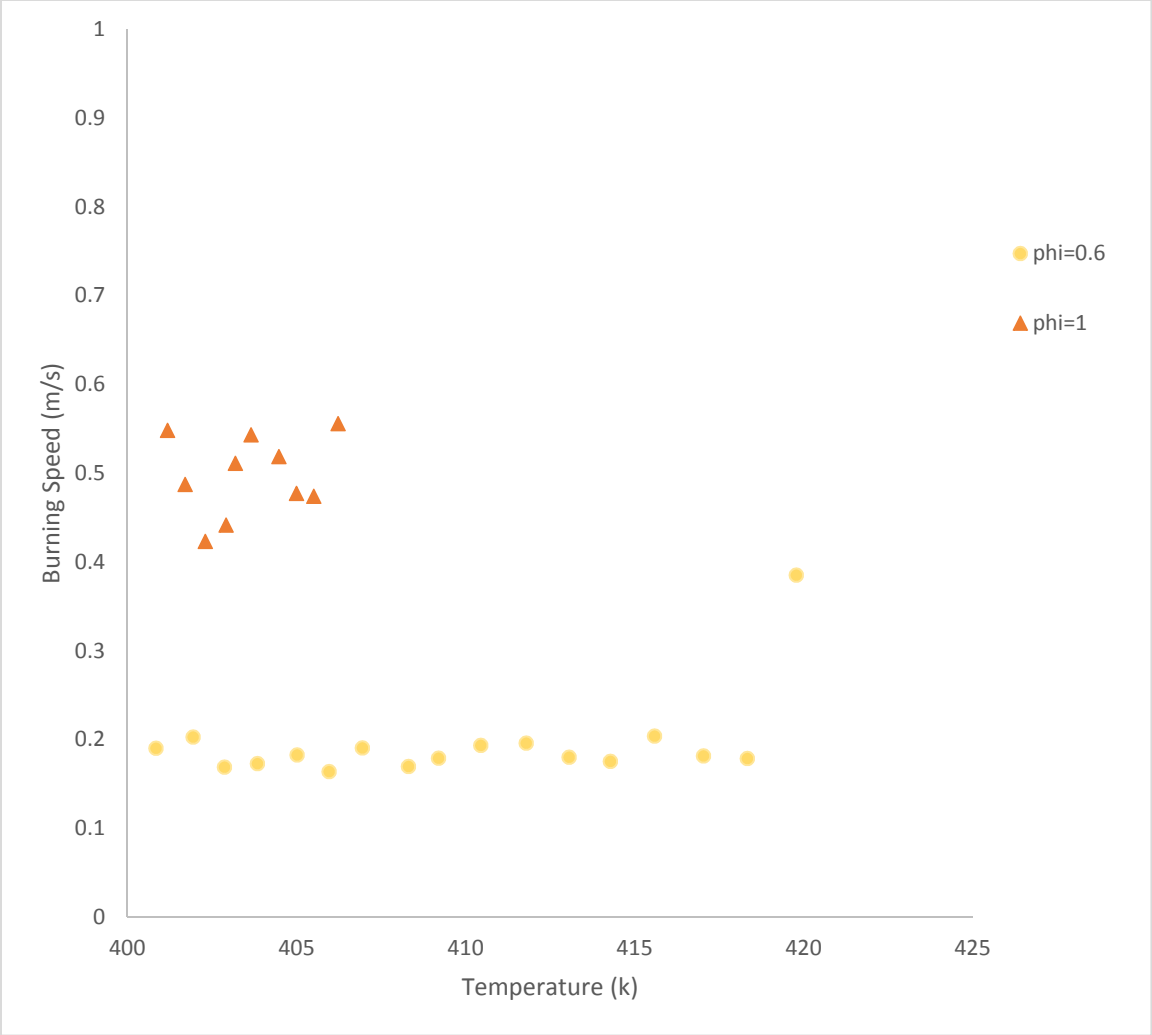

Figure 20: Laminar burning speeds of syngas/air mixture along an isentrope with initial temperature of 380 K, initial pressure of 2.0 atm and fuel air equivalence ratio ranging from 0.6 to 5.

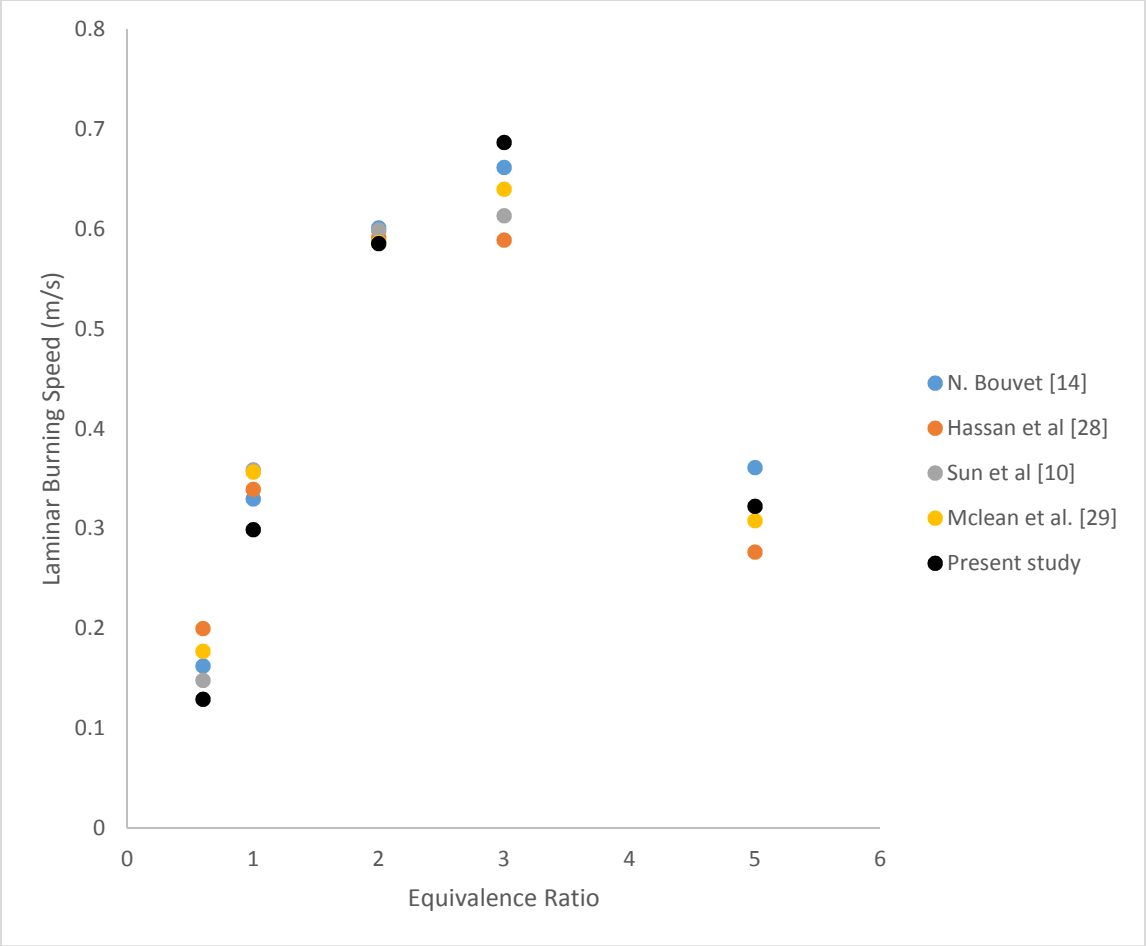

Figure 21: Laminar burning speed comparison with researchers' results.